Neuroscience 560 (2024) 181–190

Contents lists available at ScienceDirect

Neuroscience

journal homepage: www.elsevier.com/locate/nsc

# Therapeutic potential of astrocyte-derived extracellular vesicles in mitigating cytotoxicity and transcriptome changes in human brain endothelial cells

Ruth Stewart, K. Hope Hutson, Gergana G. Nestorova*

*School of Biological Sciences, Louisiana Tech University, Ruston, LA, 71270, USA*

ARTICLEINFO

*Keywords:*
Blood-brain barrier
Extracellular vesicles lncRNA
Neurodegeneration
8OHdG

ABSTRACT

This study investigates the therapeutic effect of astrocyte-derived extracellular vesicles (EVs) in mitigating neurotoxicity-induced transcriptome changes, mitochondrial function, and base excision repair mechanisms in human brain endothelial cells (HBECs). Neurodegenerative disorders are marked by inflammatory processes impacting the blood–brain barrier (BBB) that involve its main components- HBECs and astrocytes. Astrocytes maintain homeostasis through various mechanisms, including EV release. The effect of these EVs on mitigating neurotoxicity in HBECs has not been investigated. This study assesses the impact of astrocyte-derived EVs on global transcriptome changes, cell proliferation, cytotoxicity, oxidative DNA damage, and mitochondrial morphology in HBECs exposed to the neurotoxic reagent $Na_2Cr_2O_7$. Exposure to $Na_2Cr_2O_7$ for 5 and 16 h induced oxidative DNA damage, measured by an increase in genomic 8OHdG, while the EVs reduced the accumulation of the adduct. A neurotoxic environment caused a non-statistically significant upregulation of the DNA repair enzyme OGG1 while the addition of astrocyte-derived EVs was associated with the same level of expression. EVs caused increased cell proliferation and reduced cytotoxicity in $Na_2Cr_2O_7$-treated cells. Mitochondrial dysfunction associated with a reduced copy number and circular morphology induced by neurotoxic exposure was not reversed by astrocyte-derived EVs. High-throughput RNA sequencing revealed that exposure to $Na_2Cr_2O_7$ suppressed immune response genes. The addition of astrocyte-derived EVs resulted in the dysregulation of long noncoding RNAs impacting genes associated with brain development and angiogenesis. These findings reveal the positive impact of astrocytes-derived EVs in mitigating neurotoxicity and as potential therapeutic avenues for neurodegenerative diseases.

## Introduction

Neurodegenerative diseases, including Alzheimer's, Parkinson's, amyotrophic lateral sclerosis, and Huntington's, manifest as progressive neuronal damage, resulting in diminished motor function and cognitive decline. Emerging evidence highlights the role of oxidative stress- induced neural cell damage in the development of these neurodegenerative disorders. Reactive oxygen species (ROS) selectively target critical macromolecules within the brain, including lipids, proteins, and nucleic acids, that lead to impairment of physiological functions (Collin, 2019). ROS is associated with the accumulation of DNA base modifications and the formation of single and double-strand breaks. An elevated level of oxidative stress is a major factor in the development of various neurodegenerative diseases (Singh et al, 2019). Cellular ROS are generated from both exogenous and endogenous sources. Exogenously, ROS can be produced through exposure to ultraviolet and ionizing radiation, as well as various drugs, environmental toxins, and chemicals (Kim et al, 2015). The endogenous generation of ROS is caused by mitochondrial and non-mitochondrial ROS-generating enzymes. These enzymes, including nicotinamide adenine dinucleotide phosphate oxidase, xanthine oxidase, cytochrome P450, and flavin oxidases, play a crucial role in the regulated production of ROS as part of normal cellular processes. The disruption of the equilibrium between ROS production and antioxidant defenses leads to oxidative stress that contributes to the development and progression of neurodegenerative diseases (Song and Zhou, 2015).

8-hydroxy-2 -deoxyguanosine (8OHdG), an oxidized form of guanine, is a biomarker for the assessment of oxidative stress and carcinogenesis (Valanidis et al., 2009). Unrepaired 8OHdG induces mutagenesis and carcinogenesis (Cooke et al., 2003). 8-Oxoguanosine DNA glycosylase-1 (OGG1) is the enzyme responsible for excising 8OHdG through the base excision repair pathway (Boiteux et al., 2000). The gene expression

* Corresponding author at: Louisiana Tech University, 1 Adams Blvd., PO 3179, Ruston, LA, 71720, USA. *E-mail address:* ggnestor@latech.edu (G.G. Nestorova).

https://doi.org/10.1016/j.neuroscience.2024.09.040 Received 15 March 2024; Accepted 20 September 2024 Available online 27 September 2024

levels of OGG1 decrease in human astrocytes and A549 lung carcinoma cells when exposed to sodium dichromate, suggesting a correlation between OGG1 expression and oxidative DNA damage (Hodges and Chipman, 2002). Brain cells are continuously challenged by ROS, and effective neuronal repair of ROS-induced 8OHdG accumulation is critical to maintaining brain function and reducing the rate of C: G to A: T transversion mutation. The blood–brain barrier (BBB) is a highly specialized and selective physiological barrier that separates the bloodstream from the central nervous system. It plays a crucial role in maintaining the brain's homeostasis and protecting it from potentially harmful substances. Human brain endothelial cells (HBEC), along with astrocytes and pericytes, play a key role in forming and maintaining the BBB (Abbott et al., 2010). The intercellular communication between HBEC and astrocytes is crucial for the proper functioning and maintenance of the BBB, as well as various neurological processes. Astrocytes release signaling molecules that induce the differentiation of HBEC, modulate the immune response and BBB integrity, and provide metabolic support and neuroprotection (Abbott et al., 2006).

Extracellular vesicles (EVs) are particles released from cells that have a lipid bilayer and cannot replicate independently (Welsh et al., 2024). They encapsulate nucleic acids, proteins, and lipids that can be transferred to recipient cells to influence physiological responses (Lee and Kim, 2017; Upadhya et al., 2020. These nanosized vesicles serve as a source of genomic and proteomics biomarkers and play a role in the progression of neurodegenerative diseases (Hill, 2019). Microglia- derived EVs play a crucial role in the Amyloid Beta (Aβ) and tau propagation in Alzheimer's disease (Lee et al., 2019). Blood and cerebrospinal fluid-derived EVs from individuals with Amyotrophic Lateral Sclerosis show enrichment for inflammatory RNA and protein biomarkers (Barbo & Ravnik-Glava˘c, 2023). Microglia-derived EVs contribute to the aggregation and spread of α-syn in the brain of Parkinson's disease patients (Guo et al., 2020). Prion-infected cells release extracellular vesicles containing cellular prion proteins and mitochondrial fragments, serving as biomarkers for this neurological disease (Khadka et al., 2023). Due to their nano-size, EVs can cross the BBB, but with low efficiency (Shi et al., 2014).

Astrocyte-derived EVs encapsulate neuroglobin, suggesting their potential role as vehicles for transferring neuroprotective factors to neurons (Venturini et al., 2019). Apurinic/apyrimidinic endodeoxyribonuclease 1 (APE1), the main AP-endonuclease of the DNA base excision repair pathway, is enzymatically active in EVs (Mangiapane et al., 2021). Long noncoding RNAs (lncRNA) are encapsulated in EVs and facilitate the exchange of epigenetic information (Dragomir et al., 2018). Several astrocytes EV-derived lncRNA have been conformed to affect neuronal and microglia function. The long noncoding RNA 4933431K23Rik enhanced post-traumatic recovery and cognitive function by targeting microglial activation (He et al., 2023). Astrocyte EV- derived lincRNA-Cox2 enhanced microglial phagocytosis and contributed to the maintenance of homeostasis (Hu et al., 2018). Astrocyte- derived EVs facilitate the transfer of lncRNA NKILA into neurons, resulting in increased proliferation and reduced apoptosis. This mechanism promotes brain recovery following traumatic brain injury (He et al., 2021). However, the effect of astrocyte-derived EV on HBEC remains unexplored.

The main goal of this in vitro study is to assess the therapeutic potential of astrocyte-derived EVs on HEBCs. This work investigates the impact of EVs on the transcriptome changes, base excision repair capabilities, and mitochondrial function of HBECs treated with the toxic reagent $Na_2Cr_2O_7$. Our findings indicate that astrocyte-derived EVs transfer nucleic acids and proteins that change the lncRNA expression profile of the recipient HEBC and offer protection against ROS.

**Experimental Procedures**

*Human astrocytes and human brain endothelial cell culture*

Human astrocytes (ScienCell, Carlsbad, CA, #1800) were cultured in 100 mm Petri dishes coated with poly-L-lysine, containing 12 mL of Astrocyte Medium (ScienCell, #1801), supplemented with 1 % penicillin/streptomycin solution (ScienCell, #0503), 2 % Fetal Bovine Serum (ScienCell, #0500), and 1 % astrocyte growth supplement (ScienCell #1852). Cultures were maintained at 37 °C, 95 % humidity, and 5.0 % CO2/air until reaching 80 % confluence. Subculturing was performed with a uniform seeding density of $2.2 \times 10^6$ cells per petri dish using the Countess II FL Automated Cell Counter (ThermoFisher Scientific, Waltham, MA). Human brain endothelial cells (AddexBio, San Diego, CA, #T0005011) were cultured in 100 mm Petri dishes coated with 0.1 % gelatin, containing 12 mL of DMEM/F12 Endothelial Cell Medium (ThermoFisher, Waltham, MA, # 11320033) supplemented with 40 μg $mL^{-1}$ Endothelial Cell Growth supplement (Corning, Glendale, AZ, #354006) and 10 % Fetal Bovine Serum (Gibco, # A3160501). Cultures were seeded at $1.2 \times 10^6$ seeding density, maintained at 37 °C, 95 % humidity, and 5.0 % $CO_2$/air until reaching 80–90 % confluence. The HEBCs were treated with 10 μM and 100 μM $Na_2Cr_2O_7$, with and without EVs, and incubated for 5 h and 16 h followed by purification of RNA, DNA, MTT, and ROS assays. Nontreated cells were maintained in parallel as a control.

*Astrocytes-derived EV purification, protein characterization, and size distribution analysis*

Human astrocyte cell cultures were grown until reaching 80–90 % confluency. Polymer-precipitation reagent (Total Cell Culture Exosomes Isolation, Thermo Fisher Scientific, #4478359) was used to isolate EVs from 10 mL of astrocytes-conditioned cell media. The EVs were stored at − 20 °C in a PBS buffer for further analysis. Before protein quantification, the EVs were lysed by adding 50 μL RIPA lysis buffer (Thermo Fisher Scientific, cat.89900) to 2 μL of EVs followed by 15 min of incubation on ice. The protein concentration was measured using the Pierce BCA Protein Assay Kit (ThermoFisher Scientific, Cat. #23225). The concentrations of CD63 and calnexin were measured using a Human CD63 ELISA kit (Cat. #A310656, Antibodies, USA) and a Human Calnexin ELISA kit (Cat. #A312799, Antibodies, USA), respectively, following the manufacturer's guidelines. The assays were performed using 10 μg of protein equivalent from lysed and intact EVs per well. A standard curve provided by the manufacturer was generated for each experiment to determine protein concentrations. Each experimental group included six replicates. A *t*-test was conducted to assess the statistical significance between the experimental groups. The intact EVs' size distribution and concentration were determined using a NanoSight Pro Nanoparticle analyzer (Malvern Panalytical, UK). The sample was diluted with room temperature DPBS in a 1:1 ratio before particle analyses and the analysis was performed with 5 technical replicates (5 captures) using a light scatter filter (532 nm laser wavelength). The treatment used $4.43 \times 10^6$ EVs equivalent to 747 μg of protein per well.

*Assessment of ROS levels, cell proliferation and cytotoxicity*

ROS levels were assessed using the ROS Detection Assay kit (OZ BioSciences, San Diego, CA, # ROS0300). Human brain endothelial cells were cultured in gelatin-coated 96-well plates and treated with 10 μM and 100 μM of $Na_2Cr_2O_7$ for 5 h in the presence and absence of astrocyte- derived EVs. Non-treated cells served as baseline control and each experimental group consisted of eight biological replicates. The positive control, *tert*-butyl hydrogen peroxide (TBHP), was added following the manufacturer's protocol. ROS levels for each treatment condition were quantified using an Infinite® 200 Pro microplate reader with ex485/ em535 (Tecan, USA). The cell viability and cytotoxicity in the experimental groups were evaluated using the MTT Cell Proliferation Assay Kit (Abcam, Cambridge, UK, # Ab211091). The results were quantified by measuring absorbance at 450 nm with a MultiSkan Go (Thermo Scientific, USA) and absorbance measurements were proportional to the cell number in each well. The cytotoxicity for each experimental group represents a percent change between the average absorbance of the untreated and treated experimental groups.

*8OHdG genomic levels*

The Human brain endothelial cells were treated with 100 µM and 10 µM $Na_2Cr_2O_7$ for 5 h and 16 h in the presence and absence of astrocytes- derived EVs. The DNA was collected and purified using Monarch Genomic DNA Purification Kit (New England BioLabs, Ipswich, MA, #T3010S) following the manufacturer's protocol. The DNA was quantified with the Qubit DNA Broad Range Assay Kit (Invitrogen, Waltham, MA, #Q33265), and 100 ng of DNA was used per well. The concentration of genomic 8-OHdG was assessed using ELISA using an EpiQuick 8- OHdG DNA damage quantification kit (EpienTek, Farmingdale, NY, cat. P-6004). Each experimental group comprised three biological replicates, each representing the average of two technical replicate measurements.

*RT-qPCR analysis of OGG1mRNA expression in HBECs*

Total RNA from sodium dichromate-treated HBECs for 5 h and 16 h in the presence or absence of astrocytes-derived EVs was extracted and purified using the Monarch Total RNA Miniprep Kit (New England BioLab, Ipswich, MA, # T2010S). The RNA concentration was quantified with the Qubit RNA Broad Range Assay Kit (Invitrogen, Waltham, MA, # Q102100). TaqMan™ RNA-to-CT™ 1-Step Kit (ThermoFisher Scientific, cat.4392653) was utilized to measure OGG1 expression. TaqMan™ Gene Expression Assay (FAM) (ThermoFisher Scientific, USA) specific for OGG1 was employed. Equal amounts of RNA (9 ng) were combined with 10 µl of TaqMan® RT-qPCR mix, 1 µl of TaqMan® Gene Expression Assay, 0.5 µl of TaqMan® RT Enzyme Mix, and RNAse-free H2O. Amplification was conducted following the manufacturer's instructions using the QuantStudioTM 3 Real-time PCR system (Applied Biosystems, Waltham, MA, Cat. # A28567). Data analysis was performed using GraphPad Prism 6 (GraphPad Software, La Jolla, USA). The results, presented as mean ± standard error, were calculated from three biological replicates, each including three technical replicates. *Fluorescence analysis of mitochondria morphology and copy number*

For mitochondria analysis, HBECs were cultured in a 96-well plate and treated with 10 µM and 100 µM $Na_2Cr_2O_7$ for 5 h and 16 h. After the incubation, the nucleus of the cells was stained with DAPI (Invitrogen, #D1306), and the mitochondria were labeled with MitoTracker Green FM Dye (Invitrogen, #M7514) following the manufacturer's protocol. The nucleus of the cells was stained with Hoechst Nucleic Acid Stain (ThermoFisher Scientific, cat. H3570). The fluorescent images were obtained using Invitrogen™ EVOS™ FL Digital Inverted Fluorescence Microscope (ex./em. 490/516 nm and 350/460) and processed using FIJI/Image J following the pipeline protocol for mitochondria morphology and networking quantification described by Chaudhry et al., 2020. The mitochondria fluorescence was quantified using an Infinite® 200 Pro microplate reader with ex/em 485/535 (Tecan, USA). Each experimental group included eight biological replicates.

*RNA sequencing of untreated and 10 µM $Na_2Cr_2O_7$ treated cells in the presence and absence of astrocytes-derived EVs*

Total RNA from three HBEC groups (untreated, 10 µM $Na_2Cr_2O_7$ treated with astrocytes-derived EVs, and without EVs) was purified using the Quick-DNA/RNA MicroPrep Plus Kit (Zymo Research, Orange, CA, #D7005). Each experimental group included three biological replicates. The RNA was quantified using a Qubit RNA BR assay kit (Invitrogen, #2216946). TruSeq® Stranded Total RNA Library Prep kit (Illumina, San Diego, CA, cat. #20020596) was used for library preparation using 1 µg of RNA per sample. Libraries were quantified and normalized to 4 nM and then diluted to 2 pM. An internal control, a 5 % library of 2 pM PhiX, was spiked in. Sequencing was performed on an Illumina NextSeq 550 platform, generating an output of up to 400 M reads per sample. Base calling and quality scoring were conducted using Illumina Data Analysis Software. The T-Bioinfo server pipeline (Pine Biotech, New Orleans, LA) was used for read grouping, alignment, and gene expression quantification, and provided a list of differentially expressed genes. Bowtie-2 algorithm was used for alignment of the reads to the reference Homo Sapiens genome. The Sailfish algorithm was employed to determine the transcript counts within each group and $\log_2$ gene expression between the experimental groups. Statistically significant differentially expressed genes with a fold change greater or less than 2.0 were subjected to pathway enrichment analysis using the GO enrichment tool GOrilla (Eden et al., 2009). GOrilla compared the target gene list to a background set to assess the significance of the enrichment for previously annotated GO terms.

**Results**

*Astrocytes-derived EVs reduce ROS and cytotoxicity and increase proliferation in HBEC treated with $Na_2Cr_2O_7$*

The average size of the astrocytes-derived EVs was 196 nm, the mode was 152 nm and the concentration was $4.43 \times 10^8$ EV $ml^{-1}$ (Fig. 1a). The protein content-based characterization of EVs revealed the presence of the transmembrane EV marker CD63, localized on the outer surface of the vesicles (Fig. 1b). The assessment of soluble proteins associated with intracellular compartments indicated the presence of calnexin, a protein associated with the endoplasmic reticulum and Golgi apparatus secretory pathways (Fig. 1c) (Welsh et al., 2024). Calnexin enrichment has been specifically linked to larger EVs within the 100–400 nm size range (Saludas et al., 2022). Treatment with 10 µM and 100 µM $Na_2Cr_2O_7$ for 5 h resulted in a non-statistically significant elevation in ROS levels and reduced proliferation in HBECs. The co-administration of astrocyte- derived EVs during the treatment mitigated the adverse effects on the cells (Fig. 1d and 1e). The ROS assay uses a fluorogenic probe that diffuses into the cells, becoming fluorescent upon ROS-mediated oxidation. The average fluorescent intensity correlates with cellular ROS levels and the cell count in each well. Cytotoxicity analysis using the MTT assay confirmed a concentration-dependent increase in cytotoxicity associated with $Na_2Cr_2O_7$. The addition of EVs resulted in a reduction a reduction in cytotoxicity (Fig. 1f).

*Astrocytes-derived EVs and oxidative DNA damage of HEBCs*

Exposure to the neurotoxic chemical $Na_2Cr_2O_7$ is associated with a dose-dependent increase in genomic levels of 8OHdG. Following a 10 µM treatment, changes in 8OHdG were minimal. Increasing the concentration to 100 µM leads to a substantial 8OHdG increase of 200 % and 254 % after 5 and 16 h of exposure, respectively (Fig. 2a, b). The positive effect of astrocyte-derived EVs on oxidative DNA damage of HEBC can be observed after 5 h of exposure to a toxic environment. The genomic levels of 8OHdG were reduced by 50 % after 5 h and no difference was observed after 16 h of treatment with 10 µM $Na_2Cr_2O_7$. This accumulation of 8OHdG was not affected when the concentration of the toxic reagent was increased (Fig. 2 a,b). Our findings align with previous studies, confirming a positive correlation between Cr toxicity and 8OHdG levels. This relationship is reversed in the presence of the antioxidative reagent glutathione and the ROS scavenger ascorbate (Kart et al., 2016; Tsou et al., 1996). These results underscore the potential therapeutic role of astrocyte-derived EVs in reducing HBEC oxidative DNA damage induced by exposure to a toxic environment. The levels of

**Fig. 1.** Size distribution of EVs and the effect of astrocyte-derived EVs on HBEC treated with $Na_2Cr_2O_7$. (a) Size distribution of astrocytes-derived EVs; (b) Concentration of tetraspanin CD63 in lysed and intact EVs derived from astrocytes, with 10 µg of protein equivalent per well; six biological replicates. (c) The concentration of calnexin in lysed and intact EVs derived from astrocytes, with 10 µg of protein equivalent per well; six biological replicates; (d) Reactive oxygen species measurements in untreated HBEC and cells exposed to 10 µM and 100 µM $Na_2Cr_2O_7$ for 5 h, both in the presence (EV + ) and absence (EV-) of astrocyte-derived EVs. The positive control, TBHP, is a ROS-inducing reagent. (e) Assessment of MTT cell proliferation and metabolic activity in untreated HBEC cells exposed to 10 µM and 100 µM $Na_2Cr_2O_7$ for 5 h, with and without astrocyte-derived EVs. (f) Evaluation of the cytotoxic effects of 5-hour treatment with 10 µM and 100 µM $Na_2Cr_2O_7$ on HBEC, comparing the effect in the presence and absence of EVs. Eight biological replicates were included in each experimental group. The error bars represent the

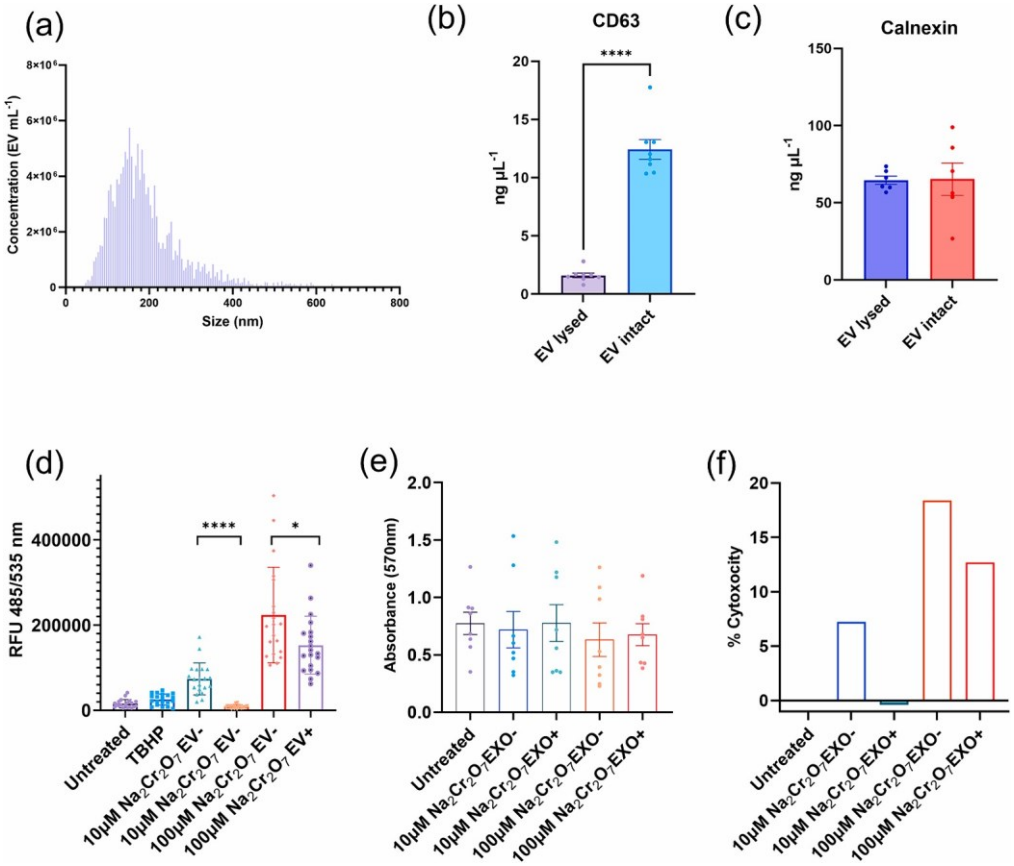


SEM and the statistical analysis was performed using a *t*-test.

OGG1 mRNA expression were evaluated to investigate a correlation with the observed changes in 8OHdG concentration. While exposure to the reagent led to an increase in OGG1 expression in the absence of EVs, these results are not statistically significant. The presence of astrocyte- derived EVs was associated with a lack of upregulation of OGG1 (Fig. 2 c, d). Other studies conducted using human astrocytes revealed a non-statistically significant decrease in both OGG1 mRNA and protein expression following treatment with 10 µM sodium dichromate. (Nwokwu, 2022). Exposure of lung carcinoma cells to reagent inhibited OGG1 expression at doses exceeding 25 µM (Hodges and Chipman, 2022). These findings suggest complex regulatory mechanisms involving EVs and cellular responses to toxic insults, highlighting the need for analysis of involved pathways in the context of oxidative stress.

*Fluorescent analysis of mitochondrial morphology*

MitoTracker™ Green, a cell-permeable probe, passively diffuses across the plasma membrane and accumulates within active mitochondria. The increase in fluorescence signal is proportional to the size or the number of mitochondria per cell. Fluorescence-based analysis indicated a statistically significant decrease in fluorescence following exposure to $Na_2Cr_2O_7$. The increase in mitochondria-associated signal was not statistically significant upon the addition of astrocyte-derived EVs (Fig. 3a). A multidimensional analysis of mitochondria was performed using fluorescence microscopy imaging and the open-source image analysis platform ImageJ. The results indicated a dose and time-dependent reduction in HBECs mitochondrial copy number in response to $Na_2Cr_2O_7$ exposure. EVs didn't have a statistically significant effect on the change of mitochondria (Fig. 3b). The aspect ratio measured as the length-to-width ratio was assessed to characterize mitochondrial health. Increased exposure time and higher $Na_2Cr_2O_7$ concentration resulted in an aspect ratio decrease which is indicative of fission and fragmentation, associated with mitophagy (Park et al., 2012). The addition of EVs in the presence of toxic reagents didn't cause a statistically significant change in the aspect ratio of mitochondria (Fig. 3c). Fluorescent images of the stained mitochondrial networks within the HEBC are shown in Fig. 3d. These images show the overall effect of the $Na_2Cr_2O_7$ and EVs treatment on the cellular morphology.

*High throughput RNA sequencing: Suppression of immunoregulation following $Na_2Cr_2O_7$ treatment and lncRNA-mediated transcriptome regulation via astrocyte-derived EVs*

RNA sequencing analysis revealed distinct read counts and mapping efficiencies across experimental groups. The average number of reads in the untreated group was 69,648,986. In the absence of EVs, the treated group had an average of 48,178,445 reads, while in the presence of EVs, the average reads were 39,179,927. The mapping efficiencies, expressed as the percentage of reads successfully aligned to the reference human genome were high among all experimental conditions. The untreated

**Fig. 2.** Assessment of oxidative DNA damage and OGG1 mRNA expression in HBEC. Genomic levels of 8OHdG were measured in HBEC subjected to 10 µM and 100 µM $Na_2Cr_2O_7$ treatment, both in the presence and absence of astrocyte-derived EVs, for (a) 5 h and (b) 16 h. The OGG1 gene expression was analyzed after treatment for (c) 5 and (d) 16 h with 10 µM and 100 µM $Na_2Cr_2O_7$. 8OHdG genomic concentration was determined using ELISA, while OGG1 mRNA expression was assessed via RT-qPCR. Each experimental group includes six biological and two technical replicates. The error bars represent the SEM and the statistical analysis was performed using a *t*-test.

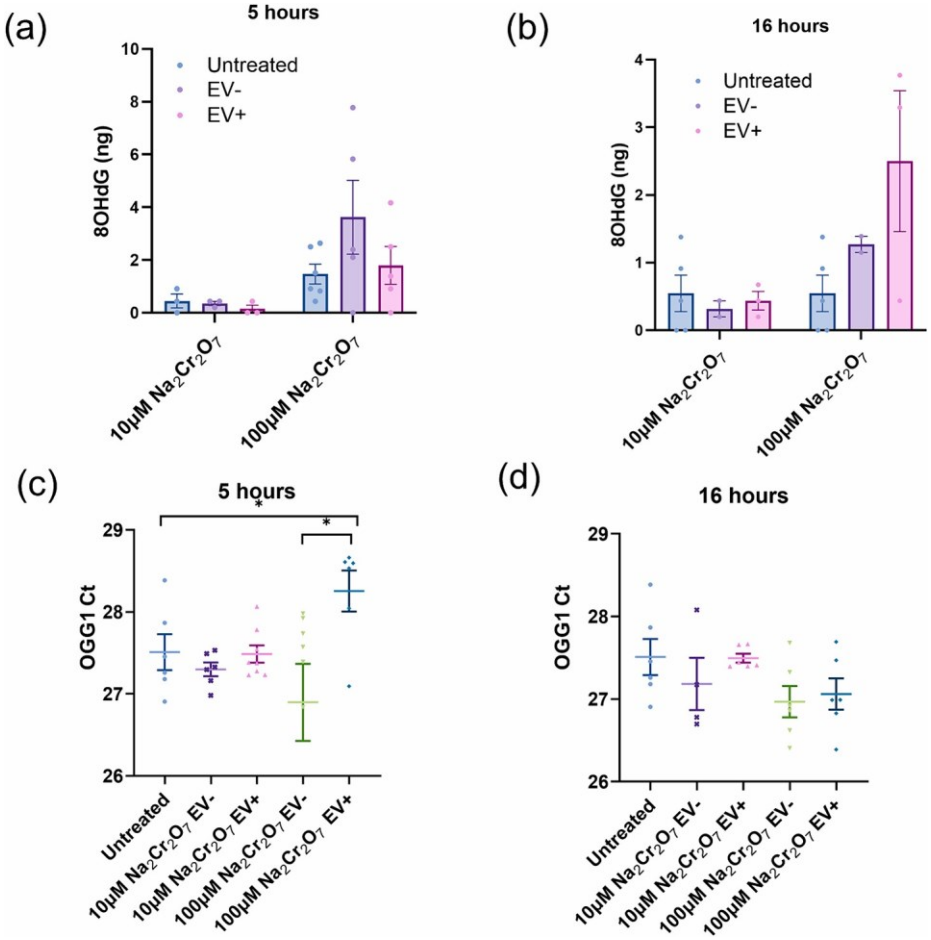


group has a mapping efficiency of 98.7 %. In the 10 µM $Na_2Cr_2O_7$- treated groups with and without EVs, 98.1 % and 96.7 % of the reads aligned to the reference genome. Differential expression analysis was performed to investigate the effect of the sodium dichromate treatment and the global transcriptome changes in the HEBCs induced by astrocytes-derived EVs. A significant number of genes were statistically significantly dysregulated following 5 h exposure to 10 µM sodium dichromate (Fig. 4a). A smaller subset of genes were up and downregulated due to the EV transfer of genetic cargo (Fig. 4b). A heatmap, visually representing the top upregulated and downregulated genes between the treated and untreated experimental groups (Fig. 4c), revealed distinct expression patterns between the conditions. The majority of genes exhibited an opposite expression trend following exposure to 10 µM $Na_2Cr_2O_7$, highlighting the impact of the treatment on the expression of multiple genes.

The GO enrichment analysis was conducted on the statistically significant ($p < 0.05$) differentially expressed genes with a fold change greater than or less than 2.0, between untreated human endothelial brain cells and those treated with 10 µM $Na_2Cr_2O_7$ (supplementary Table 1). The enriched GO terms included the Biological Processes, Cellular Components, and Molecular Function categories. The analysis revealed a significant downregulation of genes associated with the regulation of immune system processes (GO:0002682), a decrease in response to external biotic stimuli (GO:0043207), reduced cellular defense (GO:0006952), inflammatory (GO:0006954), and immune (GO:0006955) responses (Fig. 5a). The downregulation of chemokine (GO:0008009) and cytokine (GO:0005125) activities, as well as chemokine (GO:0042379) and CCR chemokine receptor binding (GO:0048020), suggest a disruption of immune surveillance and inflammatory processes (Fig. 5b). The RNA sequencing analysis indicated a significant upregulation in gene expression related to plasma membrane-associated functions after treatment with 10 µM $Na_2Cr_2O_7$. The enriched GO terms in the cellular components' category indicate an increase in the activity of integral membrane proteins (Fig. 5c).

Comparison of the gene expression between the treated groups in the presence or absence of astrocytes-derived EVs revealed that the majority of the dysregulated genes are lncRNAs (supplementary Table 2). Most of the lnCRNA were transcripts that were not characterized yet. Recent studies have found that two of the dysregulated lncRNAs, namely LMCD1-AS1 and ADAMTS9-AS1, can target four different genes, including COL6A3 (Yu et al., 2019), P4HA2 (Wang et al., 2019), miR- 106b-5p (He et al., 2020), and PRDM16 (Wu et al., 2023). The identified target genes play diverse roles in cellular processes, ranging from extracellular matrix maintenance (COL6A3 and P4HA2) (Zanotti et al., 2023; Myllyharju, 2003) to microRNA-mediated regulation (miR-106b- 5p) and transcriptional modulation of neurogenesis (PRDM16) (He, et al., 2021). The GO enrichment analysis of the statistically significant downregulated genes following EV treatment reveals an impact on key biological processes within the brain that include axon guidance, responses to bone morphogenic protein (BMP) signaling, and cell

**Fig. 3.** Fluorescence imaging of mitochondria and quantitative analysis of mitochondrial morphology. (a) Fluorescence plate reader assessment of MitoTracker™ Green dye accumulation in HBECs following exposure to sodium dichromate, with and without astrocyte-derived EVs. (b) Dose-dependent reduction in mitochondrial copy numbers per cell upon $Na_2Cr_2O_7$ exposure, mitigated by astrocyte-derived EVs at a lower dose (10 μM). (c) Aspect ratio measurement, indicating changes in mitochondrial elongation or circularity, with astrocyte-derived EVs promoting a healthier and more interconnected mitochondrial network. Each experimental group included eight biological replicates. The results are presented as the mean+/- SEM and the statistical analysis was performed using a *t*-test. (d) Fluorescent images of labeled mitochondria, scale bar is 200 μm. The images correspond to the following experimental groups: (i) 5 h untreated; (ii) 5 h 10 μM $Na_2Cr_2O_7$ EV-; (iii) 5 h 10 μM $Na_2Cr_2O_7$ EV+; (iv) 5 h 100 μM $Na_2Cr_2O_7$ EV-; (v) 5 h 100 μM $Na_2Cr_2O_7$ EV+; (vi) 16 h untreated; (vii) 16 h 10 μM $Na_2Cr_2O_7$ EV-; (viii) 16 h 10 μM $Na_2Cr_2O_7$ EV+; (ix) 16 h 100 μM $Na_2Cr_2O_7$ EV-; (x) 16 h 100 μM $Na_2Cr_2O_7$ EV+; (For interpretation of the references to colour in this figure legend, the reader is referred to the web

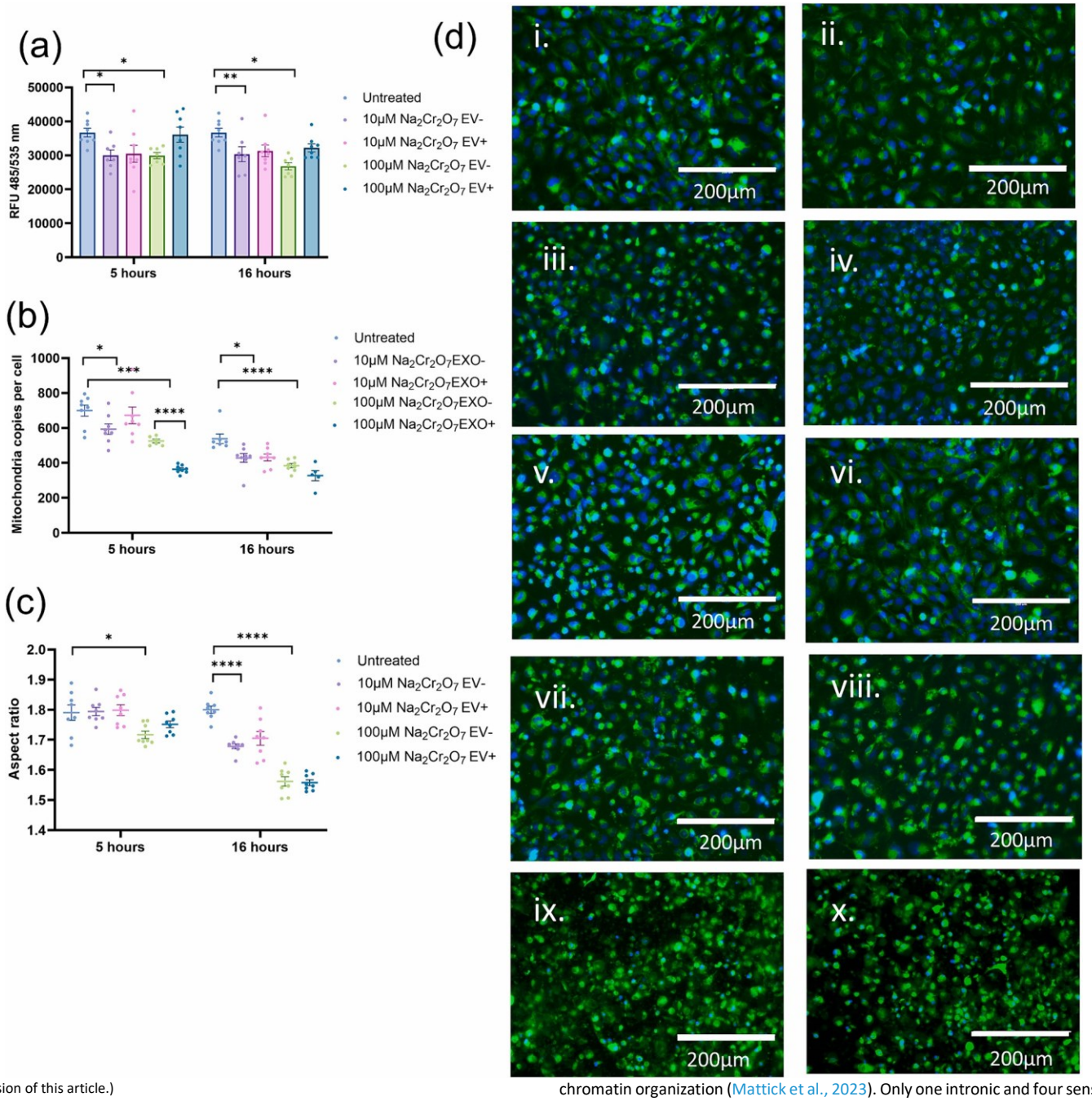


version of this article.)

differentiation (Fig. 6a). These findings provide insights into the specific molecular pathways and regulatory mechanisms in HBEC that are induced by EV-derived cargo. The functional classification of differentially expressed lncRNA types of post-EV treatment indicated predominant dysregulation in antisense and intergenic lncRNAs, comprising 90 % of the identified transcripts (Fig. 6b). These lncRNA subtypes are implicated in epigenetic and transcriptional regulations, as well as direct protein-domain interactions disrupting target protein function (Ransohoff et al., 2018). Antisense and intergenic lncRNAs regulate gene expression, alternative splicing, and chromatin organization (Mattick et al., 2023). Only one intronic and four sense lncRNAs have been statistically significantly dysregulated.

## Discussion

Astrocytes-derived EVs play a critical role in astrocytes-neuron

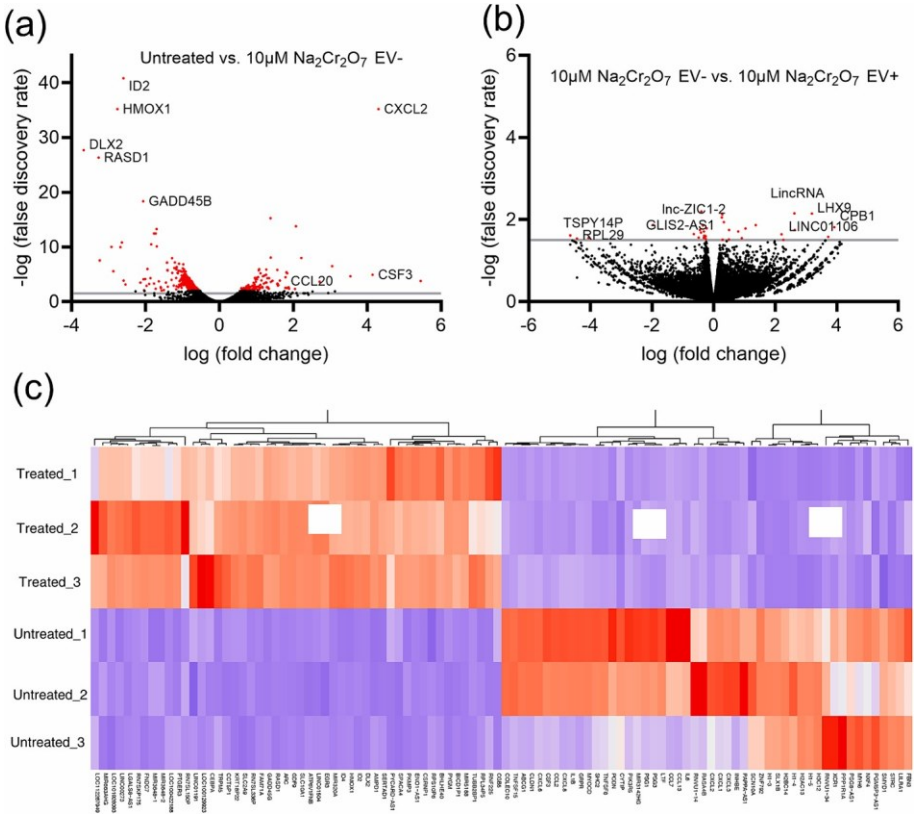


**Fig. 4.** Differential gene expression analysis of RNA sequencing results. All statistically significant genes (FDR < 0.05) were highlighted in red. (a) A volcano plot of the HEBCs differentially expressed gene after 5 h of treatment with 10 μM $Na_2Cr_2O_7$; (b) Vulcano plot of the HEBCs differentially expressed genes after incubation with astrocyte-derived EVs.; (c) Heat map cluster analysis depicting 50 up and downregulated genes between untreated and 10 μM $Na_2Cr_2O_7$-treated groups. (For interpretation of the references to colour in this figure legend, the reader is referred to the web version of this article.)

communication, promoting neurite outgrowth after stroke (Shanthi et al., 2023) and neuroprotective effects and improved motor and cognitive function in traumatic brain injury. Despite these scientific advances, the neuroprotective effects of astrocyte-derived EVs on HEBCs are not being investigated. Considering the important function of astrocytes and HEBCs in maintaining the BBB, this study aims to understand the fundamental mechanisms of EV-mediated transcriptome changes, mitochondria response, and base excision repair capabilities when the endothelial cells are exposed to a toxic environment.

Sodium dichromate, a well-characterized toxic reagent, is associated with an increase in cellular ROS through the reduction of hexavalent chromium Cr (VI) to trivalent chromium Cr (III) (Bagchi et al., 1995). The assessments of ROS levels and HBEC proliferation indicated a decrease in cellular metabolic activity and a significant increase in ROS following exposure to $Na_2Cr_2O_7$. The introduction of astrocyte-derived EVs mitigated the negative cellular impact (Fig. 1b and c). The assessment of cytotoxicity confirmed that astrocyte-derived EVs reduce apoptosis in HBECs. This suggests a protective role for astrocyte-derived EVs against the cytotoxic effects associated with $Na_2Cr_2O_7$ exposure. Other studies have shown time- and dose-dependent changes in cell viability after treatment with chromium compound. Exposure of HepG2 cells to 12.5 μM potassium dichromate led to a decrease in cell viability by 45 % and 60 % after 24 and 48 h of exposure (Patlolla et al., 2009).

Treatment with a neurotoxic reagent led to a dose-dependent increase in 8OHdG accumulation while the presence of astrocytes-derived EV was associated with a decreased genomic accumulation of the adduct at a lower concentration of the toxic reagent (Fig. 2). 8OHdG is a biomarker for oxidative DNA damage and is often used as a measure of oxidative stress at the genomic level. Elevated levels of 8OHdG indicate oxidative DNA damage and are reported to increase after Cr (IV) exposure (Kart et al., 2016). If the damage is severe and persistent, it may interfere with the normal functioning of brain endothelial cells. The cells have mechanisms for repairing DNA damage, but chronic exposure to oxidative stress may overwhelm these repair mechanisms (Valavanidis et al., 2009). An increase in the concentration or the duration of the exposure to toxic reagent could interfere with the DNA repair capabilities of the cells and therefore contribute to the insignificant effect of the EVs on the 8OHdG accumulation or OGG1 mRNA expression (Fig. 2). Oxidative stress can trigger inflammatory responses as well. In brain endothelial cells, inflammation can disrupt the tight junctions between cells, compromising the integrity of the blood–brain barrier. This could lead to increased permeability, allowing harmful substances to enter the brain. Excessive DNA damage may induce programmed cell death in brain endothelial cells that could contribute to a loss of BBB integrity and function (Galea, 2021).

The mitochondrial analysis of the sodium dichromate treated and untreated group indicated a dose-dependent reduction in both copy number and aspect ratio (Fig. 3). A lower mitochondrial count is associated with a decrease in adenosine triphosphate production and reduced cell viability (Jeng et al., 2008). The introduction of EVs counteracted this effect, contributing to an increase in the number of mitochondria per cell when exposed to lower levels of $Na_2Cr_2O_7$ (Fig. 3b). However, this mitigating effect of EVs on mitochondrial biogenesis was not evident at higher concentrations of $Na_2Cr_2O_7$. An increase in $Na_2Cr_2O_7$ concentration is associated with a further reduction in mitochondrial copies and aspect ratio, indicative of a low number of larger, more circular mitochondria with compromised function. Astrocytes-derived EVs didn't contribute to an increase in the aspect ratio that corresponds to more elongated mitochondria that could be indicative of a healthy network (van der Bliek et al., 2013). Other studies show that potassium dichromate exposure is associated with an increase in mitochondrial fission and a decrease in fusion that results in a larger

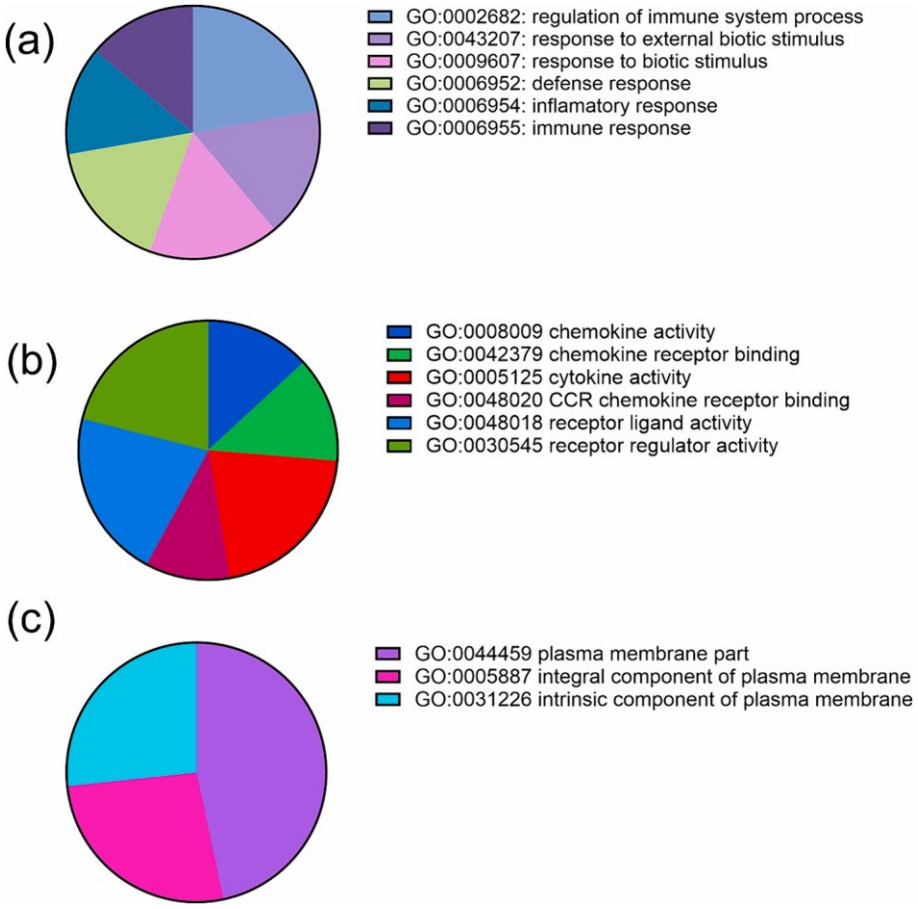


**Fig. 5.** GO functional analysis of differentially expressed genes ($p < 0.05$) in the comparison of untreated versus 10 µM $Na_2Cr_2O_7$-treated groups. The analysis provides insights into the functional implications of gene expression changes induced by 10 µM $Na_2Cr_2O_7$ treatment, highlighting key biological processes, molecular functions, and cellular components affected by exposure to a neurotoxic environment. (a) biological processes of downregulated genes; (b) molecular functions for downregulated genes; (c) cellular components of upregulated genes. The percentage of each GO category was calculated based on the number of gene hits and the total number of functional hits.

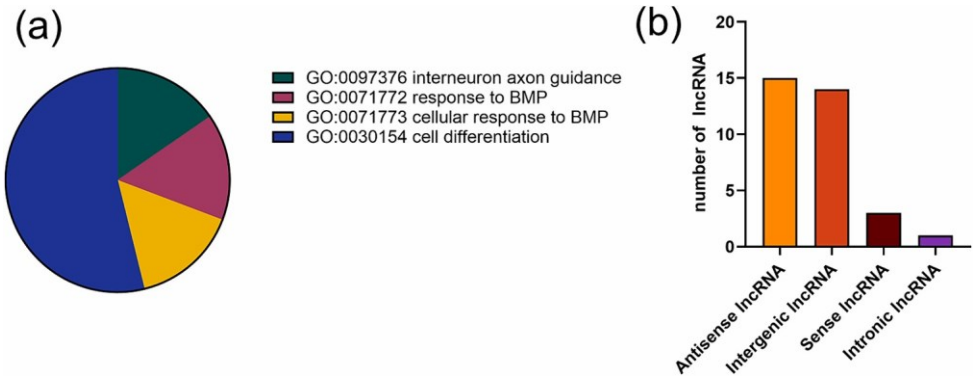


**Fig. 6.** (a) Enriched GO biological processes of upregulated genes ($p < 0.05$) upon comparison of 10 µM $Na_2Cr_2O_7$-treated groups with or without astrocyte-derived EVs. (b) Functional classification of dysregulated lncRNAs associated with astrocyte-derived EVs, with fold change < or > 1.5, $p < 0.05$.

number of fragmented mitochondria with altered permeability (Avila- Rojas et al., 2020).

High throughput transcriptome analysis was performed to identify the main biological pathways that are dysregulated after the sodium dichromate treatment and in response to the astrocytes-derived EV exposure. The downregulation of GO terms related to chemokines, cytokines, and receptor interactions impacts the inflammatory response after treatment with $Na_2Cr_2O_7$. Reduced chemokine activity impacts the recruitment and migration of immune cells to the site of inflammation.

Chemokine receptor binding is essential for signaling and immune cell responses. Downregulation of chemokine receptor binding implies a decrease in the interaction between chemokines and their receptors. Cytokines play a crucial role in regulating immune responses. Downregulation of cytokine activity may affect the modulation of inflammatory processes and immune cell activation. The downregulation of these GO terms indicates a decrease in the activity of chemokines, cytokines, and their interactions with receptors. This molecular response may have implications for regulating immune responses, immune cell recruitment, and the overall inflammatory environment within the central nervous system during neuroinflammation. The upregulation of GO terms related to the plasma membrane can have implications for neuroinflammation as well. The plasma membrane is a crucial interface between the cell and its external environment, and changes in membrane composition or structure can influence various cellular functions, including those related to immune responses and inflammation. The upregulation of

Prostaglandin E Receptor 3 (PTGER3) can mediate the effects of prostaglandin, particularly in amplifying the pro-inflammatory response (Hata and Breyer, 2004). The upregulation of IL12RB2 might contribute to the adaptive preservation of immune homeostasis. By ensuring adequate responsiveness to available IL-12, cells may attempt to regulate the balance of immune functions and prevent immune dysfunction resulting from a deficiency in key signaling molecules (Gately et al., 1998). The impact of astrocytes-derived EVs on human endothelial brain cells is evident in the modulation of gene expression, concerning key genes associated with brain development and the regulation of neural tissues. LHX9 and DLX5 genes have important roles in the differentiation and maturation of neural tissues (Peukert et al., 2011; Perera et al., 2004). An upregulation in DLX5 expression is associated with the development of brain cancer and neurological disorders (Tan and Yesta, 2021). This observation underscores the potential significance of DLX5 as a regulatory factor in pathological conditions affecting the brain. The BMP gene family is integral to various aspects of neural development, including neural induction, patterning, neurogenesis, and the proper function of the blood–brain barrier (Araya et al., 2008). BMP7, or bone morphogenetic protein 7, has a neuroprotective role in stroke animal models and promotes endogenous neurogenesis. The dysregulated genes identified in our study (supplementary Table 2) include lncRNAs with uncharacterized functions. The high-throughput sequencing analysis suggests that EVs primarily exert their neuroprotective effects through lncRNA-mediated mechanisms. The lncRNA LMCD1-AS was statistically significant downregulation following EV treatment. The validated gene targets associated with LMCD1-AS are COL6A3, P4HL, and miR-106b-5p (Bani-Yaghoub et al., 2008). Functional studies demonstrated that the depletion of LMCD1-AS1 led to suppressed cell proliferation, reduced clone formation, and inhibited invasion, while also inducing apoptosis. The LMCD1-AS1/COL6A3 axis emerged as a key player in tumorigenesis and progression, highlighting the oncogenic role of LMCD1-AS in these cellular processes (Yu et al., 2019).

While this study provides important information about the relationship between astrocyte-derived EVs and the cellular response of HEBCs, the work has several limitations. The investigation was performed using a specific concentration of EVs and therefore, may not capture the dose–response of the HEBCs. Future studies will aim to investigate a range of EV concentrations and treatment times for a more comprehensive understanding of the dose–response relationship. The cellular responses observed in an in vitro study, may not fully replicate the complex in vivo microenvironment. Incorporating in vivo models or more sophisticated in vitro systems that mimic physiological conditions could provide a more accurate representation of EV-mediated effects in a physiological context.

IIn summary, this study investigated the impact of astrocytes-derived EVs on HBEC's function including oxidative DNA damage, global transcriptome changes, and mitochondrial morphology. High throughput sequencing analysis suggests that EVs exert a neuroprotective effect via changing the expression of genes and lncRNAs that are associated with neurogenesis and neuroprotection. These findings underscore the importance of lncRNAs, particularly LMCD1-AS, in mediating the neuroprotective effects of EVs. Further investigation of the LMCD1-AS1/ COL6A3 axis and targeting this pathway in the context of neuroprotection and tumorigenesis could have implications for therapeutic interventions.

**Funding**

The study was supported by the Louisiana Space Grant Consortium (No 80NSSC20M0110) and by the NSF EPSCoR RII-Track4 grant No 2228581 and NSF MRI grant No 2320201.

**CRediT authorship contribution statement**

**Ruth Stewart:** Writing – original draft, Validation, Investigation, Formal analysis. **K. Hope Hutson:** Data curation. **Gergana G. Nestorova:** Writing – review & editing, Supervision, Resources, Project administration, Methodology, Funding acquisition, Conceptualization.

**Declaration of Competing Interest**

The authors declare that they have no known competing financial interests or personal relationships that could have appeared to influence the work reported in this paper.

**Acknowledgments**

We would like to acknowledge Thaya Stoufflet and Vladimir Chouljenko for their expert assistance with the RNA sequencing of the samples at the Louisiana State University Gene Lab and Elia Brodsky who performed the RNA sequencing gene list generation using the Pine Bio pipeline.

**Appendix A. Supplementary data**

Supplementary data to this article can be found online at https://doi.org/10.1016/j.neuroscience.2024.09.040.

**References**

Abbott, N.J., Ronnb¨ ack, L., Hansson, E., 2006. Astrocyte-endothelial interactions at the ¨ blood-brain barrier. Nat. Rev. Neurosci. 7 (1). https://doi.org/10.1038/nrn1824. Araya, R., Kudo, M., Kawano, M., Ishii, K., Hashikawa, T., Iwasato, T., Itohara, S., Terasaki, T., Oohira, A., Mishina, Y., Yamada, M., 2008. BMP signaling through BMPRIA in astrocytes is essential for proper cerebral angiogenesis and the formation of the blood-brain barrier. Mol. Cell. Neurosci. 38 (3). https://doi.org/10.1016/j. mcn.2008.04.003.

Avila-Rojas, S.H., Aparicio-Trejo, O.E., Briones-Herrera, A., Medina-Campos, O.N., Reyes-Fermín, L.M., Martínez-Klimova, E., Leon-Contreras, J.C., Hern´ andez- ´ Pando, R., Tapia, E., Pedraza-Chaverri, J., 2020. Alterations in mitochondrial homeostasis in a potassium dichromate model of acute kidney injury and their mitigation by curcumin. Food Chem. Toxicol. 145. https://doi.org/10.1016/j. fct.2020.111774.

Bagchi, D., Hassoun, E.A., Bagchi, M., Muldoon, D.F., Stohs, S.J., 1995. Oxidative stress induced by chronic administration of sodium dichromate [Cr(VI)] to rats. Comp. Biochem. Physiol. C Toxicol. Pharmacol. l 110 (3). https://doi.org/10.1016/0742- 8413(94)00103-H.

Bani-Yaghoub, M., Tremblay, R.G., Ajji, A., Nzau, M., Gangaraju, S., Chitty, D., Zurakowski, B., Sikorska, M., 2008. Neurodegenerative strategies in the brain: Emerging significance of bone morphogenetic protein 7 (BMP7). In. Biochem. Cell Biol. 86 (5). https://doi.org/10.1139/O08-116.

Barbo, M., Ravnik-Glava˘c, M., 2023. Extracellular Vesicles as Potential Biomarkers in Amyotrophic Lateral Sclerosis. Genes 14 (2). https://doi.org/10.3390/ genes14020325.

Boiteux, S., Radicella, J.P., 2000. The human OGG1 gene: structure, functions, and its implication in the process of carcinogenesis. Arch. Biochem. Biophys. 377 (1), 1–8. https://doi.org/10.1006/abbi.2000.1773.

Chaudhry, A., Shi, R., Luciani, D.S., 2020. A pipeline for multidimensional confocal analysis of mitochondrial morphology, function, and dynamics in pancreatic β-cells. Am. J. Physiol. Endocrinol. Metab. 318 (2). https://doi.org/10.1152/ ajpendo.00457.2019.

Collin, F., 2019. Chemical basis of reactive oxygen species reactivity and involvement in neurodegenerative diseases. Int. J. Mol. Sci. 20 (10). https://doi.org/10.3390/ijms20102407.

Cooke, M.S., Evans, M.D., Dizdaroglu, M., Lunec, J., 2003. Oxidative DNA damage: mechanisms, mutation, and disease. FASEB J. 17 (10). https://doi.org/10.1096/ fj.02-0752rev.

Dragomir, M., Chen, B., Calin, G.A., 2018. Exosomal lncRNAs as new players in cell-to- cell communication. Transl. Cancer Res. 7. https://doi.org/10.21037/ tcr.2017.10.46.

Eden, E., Navon, R., Steinfeld, I., Lipson, D., Yakhini, Z., 2009. GOrilla: A tool for discovery and visualization of enriched GO terms in ranked gene lists. BMC Bioinf. 10. https://doi.org/10.1186/1471-2105-10-48.

Galea, I., 2021. The blood–brain barrier in systemic infection and inflammation. Cell. Mol. Immunol. 18 (11). https://doi.org/10.1038/s41423-021-00757-x.

Gately, M.K., Renzetti, L.M., Magram, J., Stern, A.S., Adorini, L., Gubler, U., Presky, D.H., 1998. The interleukin-12/interleukin-12-receptor system: Role in normal and pathologic immune responses. Annu. Rev. Immunol. 16. https://doi.org/10.1146/ annurev.immunol.16.1.495.

Guo, M., Wang, J., Zhao, Y., Feng, Y., Han, S., Dong, Q., Cui, M., Tieu, K., 2020. Microglial exosomes facilitate α-synuclein transmission in Parkinson's disease. Brain 143 (5), 1476–1497. https://doi.org/10.1093/brain/awaa090.

Hata, A.N., Breyer, R.M., 2004. Pharmacology and signaling of prostaglandin receptors: Multiple roles in inflammation and immune modulation. In. Pharmacol. Ther. Vol. 103, Issue 2. https://doi.org/10.1016/j.pharmthera.2004.06.003.

He, J. wen, Li, D. Jian, Zhou, J. Hua, Zhu, Y. long, & Yu, B. qing. (2020). SP1-mediated upregulation of lncRNA LMCD1-AS1 functions as a ceRNA for miR-106b-5p to facilitate osteosarcoma progression. *Biochem. Biophys. Res. Commun.*, *526*(3). DOI: 10.1016/j.bbrc.2020.03.151.

He, B., Chen, W., Zeng, J., Tong, W., Zheng, P., 2021a. Long noncoding RNA NKILA transferred by astrocyte-derived extracellular vesicles protects against neuronal injury by upregulating NLRX1 through binding to mir-195 in traumatic brain injury. Aging 13 (6). https://doi.org/10.18632/aging.202618.

He, X., Huang, Y., Liu, Y., Zhang, X., Wang, Q., Liu, Y., Ma, X., Long, X., Ruan, Y., Lei, H., Gan, C., Wang, X., Zou, X., Xiong, B., Shu, K., Lei, T., Zhang, H., 2023. Astrocyte- derived exosomal lncRNA 4933431K23Rik modulates microglial phenotype and improves post- traumatic

recovery via SMAD7 regulation. Mol. Ther. 31 (5). https://doi.org/10.1016/j.ymthe.2023.01.031.
He, L., Jones, J., He, W., Bjork, B.C., Wen, J., Dai, Q., 2021b. PRDM16 regulates a temporal transcriptional program to promote the progression of cortical neural progenitors. *Development* (Cambridge) 148 (6). https://doi.org/10.1242/ dev.194670.
Hill, A.F., 2019. Extracellular vesicles and neurodegenerative diseases. In. J. Neurosci. Vol. 39, Issue 47. https://doi.org/10.1523/JNEUROSCI.0147-18.2019.
Hodges, N.J., Chipman, J.K., 2002. Down-regulation of the DNA-repair endonuclease 8- oxo-guanine DNA glycosylase 1 (hOGG1) by sodium dichromate in cultured human A549 lung carcinoma cells. Carcinogenesis 23 (1). https://doi.org/10.1093/carcin/ 23.1.55.
Hu, G., Liao, K., Niu, F., Yang, L., Dallon, B.W., Callen, S., Tian, C., Shu, J., Cui, J., Sun, Z., Lyubchenko, Y.L., Ka, M., Chen, X.M., Buch, S., 2018. Astrocyte EV-Induced lincRNA-Cox2 Regulates Microglial Phagocytosis: Implications for Morphine- Mediated Neurodegeneration. Mol. Ther. Nucleic Acids 13. https://doi.org/10.1016/j.omtn.2018.09.019.
Jeng, J.Y., Yeh, T.S., Lee, J.W., Lin, S.H., Fong, T.H., Hsieh, R.H., 2008. Maintenance of mitochondrial DNA copy number and expression is essential for the preservation of mitochondrial function and cell growth. J. Cell. Biochem. 103 (2). https://doi.org/10.1002/jcb.21625.
Kart, A., Koc, E., Dalginli, K.Y., Gulmez, C., Sertcelik, M., Atakisi, O., 2016. The Therapeutic Role of Glutathione in Oxidative Stress and Oxidative DNA Damage Caused by Hexavalent Chromium. Biol. Trace Elem. Res. 174 (2). https://doi.org/ 10.1007/s12011-016-0733-0.
Khadka, A., Spiers, J.G., Cheng, L., Hill, A.F., 2023. Extracellular vesicles with diagnostic and therapeutic potential for prion diseases. Cell and Tissue Research 392 (1). https://doi.org/10.1007/s00441-022-03621-0.
Kim, G.H., Kim, J.E., Rhie, S.J., Yoon, S., 2015. The Role of Oxidative Stress in Neurodegenerative Diseases. Exp. Neurobiol. 24 (4). https://doi.org/10.5607/en.2015.24.4.325.
Lee, J. Y., & Kim, H. S. (2017). Extracellular Vesicles in Neurodegenerative Diseases: A Double-Edged Sword. In *Tissue Eng. Regen. Med.* (Vol. 14, Issue 6). DOI: 10.1007/ s13770- 017-0090-x.
Lee, S., Mankhong, S., & Kang, J. H. (2019). Extracellular vesicle as a source of Alzheimer's biomarkers: Opportunities and challenges. In *International Journal of Molecular Sciences* (Vol. 20, Issue 7). DOI: 10.3390/ijms20071728.
Mattick, J.S., Amaral, P.P., Carninci, P., Carpenter, S., Chang, H.Y., Chen, L.L., Chen, R., Dean, C., Dinger, M.E., Fitzgerald, K.A., Gingeras, T.R., Guttman, M., Hirose, T., Huarte, M., Johnson, R., Kanduri, C., Kapranov, P., Lawrence, J.B., Lee, J.T., Wu, M., 2023. Long non-coding RNAs: definitions, functions, challenges, and recommendations. Nat. Rev. Mol. Cell Biol. 24 (6). https://doi.org/10.1038/s41580- 022-00566-8.
Myllyharju, J., 2003. Prolyl 4-hydroxylases are the key enzymes of collagen biosynthesis. Matrix Biol. 22 (1). https://doi.org/10.1016/S0945-053X(03)00006-4.
Park, S.J., Shin, J.H., Kim, E.S., Jo, Y.K., Kim, J.H., Hwang, J.J., Kim, J.C., Cho, D.H., 2012. Mitochondrial fragmentation caused by phenanthroline promotes mitophagy. FEBS Lett. 586 (24). https://doi.org/10.1016/j.febslet.2012.10.035.
Patlolla, A.K., Barnes, C., Hackett, D., Tchounwou, P.B., 2009. Potassium dichromate induced cytotoxicity, genotoxicity and oxidative stress in human liver carcinoma (HepG2) cells. Int. J. Environ. Res. Public Health 6 (2). https://doi.org/10.3390/ ijerph6020643.
Perera, M., Merlo, G.R., Verardo, S., Paleari, L., Corte, G., Levi, G., 2004. Defective neuronogenesis in the absence of Dlx5. Mol. Cell. Neurosci. 25 (1). https://doi.org/10.1016/j.mcn.2003.10.004.
Peukert, D., Weber, S., Lumsden, A., Scholpp, S., 2011. Lhx2 and Lhx9 determine neuronal differentiation and compartition in the caudal forebrain by regulating Wnt signaling. PLoS Biol. 9 (12). https://doi.org/10.1371/journal.pbio.1001218.
Ransohoff, J.D., Wei, Y., Khavari, P.A., 2018. The functions and unique features of long intergenic non-coding RNA. Nat. Rev. Mol. Cell Biol. 19 (3). https://doi.org/ 10.1038/nrm.2017.104.
Saludas, L., Garbayo, E., Ruiz-Villalba, A., Hernandez, S., Vader, P., P´ rosper, F., Blanco-´ Prieto, M.J., 2022. Isolation methods of large and small extracellular vesicles derived from cardiovascular progenitors: A comparative study. Eur. J. Pharm. Biopharm. 170, 187–196.
Shanthi, K. B., Fischer, D., Sharma, A., Kiviniemi, A., Kaakinen, M., Vainio, S. J., & Bart, G. (2023). Human Adult Astrocyte Extracellular Vesicle Transcriptomics Study Identifies Specific RNAs Which Are Preferentially Secreted as EV Luminal Cargo. *Genes*, *14*(4). DOI: 10.3390/genes14040853.
Shi, M., Liu, C., Cook, T.J., Bullock, K.M., Zhao, Y., Ginghina, C., Li, Y., Aro, P., Dator, R., He, C., Hipp, M.J., Zabetian, C.P., Peskind, E.R., Hu, S.C., Quinn, J.F., Galasko, D.R., Banks, W.A., Zhang, J., 2014. Plasma exosomal α-synuclein is likely CNS-derived and increased in Parkinson's disease. Acta Neuropathol. 128 (5). https://doi.org/ 10.1007/s00401-014-1314-y.
Singh, A., Kukreti, R., Saso, L., Kukreti, S., 2019. Oxidative stress: A key modulator in neurodegenerative diseases. Molecules 24 (8). https://doi.org/10.3390/molecules24081583.
Song, P., & Zou, M. H. (2015). Roles of Reactive Oxygen Species in Physiology and Pathology. In *Atherosclerosis: Risks, Mechanisms, and Therapies*. DOI: 10.1002/9781118828533.ch30.
Tan, Y., Testa, J.R., 2021. Dlx genes: Roles in development and cancer. Cancers 13 (12). https://doi.org/10.3390/cancers13123005.
Tsou, T.C., Chen, C.L., Liu, T.Y., Yang, J.L., 1996. Induction of 8-hydroxydeoxyguanosine in DNA by chromium(III) plus hydrogen peroxide and its prevention by scavengers. Carcinogenesis 17 (1). https://doi.org/10.1093/carcin/17.1.103.
Valavanidis, A., Vlachogianni, T., Fiotakis, C., 2009. 8-Hydroxy-2′ -deoxyguanosine (8- OHdG): A critical biomarker of oxidative stress and carcinogenesis. *J. Environ. Sci. Health C.* Environ. Carcinog. Ecotoxicol. Rev 27 (2). https://doi.org/10.1080/10590500902885684.
van der Bliek, A.M., Shen, Q., Kawajiri, S., 2013. Mechanisms of mitochondrial fission and fusion. Cold Spring Harb. Perspect. Biol. 5 (6). https://doi.org/10.1101/cshperspect.a011072.
Venturini, A., Passalacqua, M., Pelassa, S., Pastorino, F., Tedesco, M., Cortese, K., Gagliani, M.C., Leo, G., Maura, G., Guidolin, D., Agnati, L.F., Marcoli, M., Cervetto, C., 2019. Exosomes from astrocyte processes: Signaling to neurons. Front. Pharmacol. 10. https://doi.org/10.3389/fphar.2019.01452.
Wang, T., Fu, X., Jin, T., Zhang, L., Liu, B., Wu, Y., Xu, F., Wang, X., Ye, K., Zhang, W., Ye, L., 2019. Aspirin targets P4HA2 through inhibiting NF-κB and LMCD1-AS1/let- 7g to inhibit tumor growth and collagen deposition in hepatocellular carcinoma. EBioMedicine 45. https://doi.org/10.1016/j.ebiom.2019.06.048.
Welsh, J.A., Goberdhan, D.C., O'Driscoll, L., Buzas, E.I., Blenkiron, C., Bussolati, B., Cai, H., Di Vizio, D., Driedonks, T.A., Erdbrügger, U., Falcon-Perez, J.M., 2024. Minimal information for studies of extracellular vesicles (MISEV2023): From basic to advanced approaches. J. Extracellular Vesicles 13 (2), e12404.
Wu, Y., Xie, Z., Deng, S., Xia, Y., Lei, X., Yang, X., 2022. Microrna-96 In Human Cancers. J. Comb. Chem. High Throughput Screen 26 (7). https://doi.org/10.2174/1386207325666220909104803.
Yu, J., Zhang, B., Zhang, H., Qi, Y., Wang, Y., Wang, W., Wang, Y., Wang, Y., 2019. E2F1- induced upregulation of long non-coding RNA LMCD1-AS1 facilitates cholangiocarcinoma cell progression by regulating miR-345–5p/COL6A3 pathway. Biochem. Biophys. Res. Commun. 512 (2). https://doi.org/10.1016/j.bbrc.2019.03.054.
Zanotti, S., Magri, F., Salani, S., Napoli, L., Ripolone, M., Ronchi, D., Fortunato, F., Ciscato, P., Velardo, D., D'Angelo, M.G., Gualandi, F., Nigro, V., Sciacco, M., Corti, S., Comi, G.P., Piga, D., 2023. Extracellular Matrix Disorganization and Sarcolemmal Alterations in COL6-Related Myopathy Patients with New Variants of COL6 Genes. Int. J. Mol. Sci. 24 (6). https://doi.org/10.3390/ijms24065551.